Original Article
Cite This: Colloid & Nanoscience Journal 2(3) (2025) 369-381.
CNJ.araku.ac.ir

# A new combination of amino and mercapto type coupling agent to fabricate polymer-coated cobalt ferrite nanocomposite as corrosion inhibitor with high performance film-forming

**Behnia Sadat Mirhoseini[1*], Elham Allam[2]**

**Received:** 2025-02-01
**Revised:** 2025-02-11
**Accepted:** 2025-02-17
**DOI: 10.61186/CNJ.2.3.369**

[1]R&D of Water treatment, Golden Road Integrated Investment L.L.C., 111, Muscat governorate, Sultanate of Oman

[2]Alafak Institute of Information and Technology, University of Beirut, Beirut, Lebanon

## Abstract

Nanotechnology has transformed industrial corrosion limitations, offering opportunities to enhance treatment outcomes while minimizing adverse effects. This study focuses on the combination of amino and mercapto-type coupling agents to fabricate sulfonium group-containing polymer-coated cobalt ferrite nanoparticles for potential application as anti-corrosion. In this research work, two types of polymer-ferrite nanocomposite composed of a monomer comprising a sulfonium group wherein inorganic nanoparticle cores are coated by a layer comprising a copolymer of the aforesaid monomer at one end of the molecule. Two systems including a lecithin surfactant-based microemulsion system and a free lecithin emulsion system were used to synthesis nanocomposites and were labeled as PF-A and PF-B respectively. The prepared samples were characterized with X-ray Diffraction (XRD), and Dynamic Light Scattering (DLS) analysis. The prepared PF-A nanocomposite provide a forming a film having excellent anticorrosion properties on a metal surface without producing sludge, and without using phosphorus or chromium compared to PF-B in a 1.0 M HCl solution, with 100% maximum corrosion inhibition efficiency at 1.5 Wt.% of nanocomposite based on the normalized weight loss (mg/cm$^2$) measurements. The operational parameters such as temperature, and concentration of inhibitor were studied. The film forming on the surface of steel with both nanocomposite samples was confirmed with Atomic Force Microscopy (AFM) and the obtained results reveal globular nanospheres compacted and aligned near each other forming an anticorrosive shield monolayer against the corrosive environment. AFM images validate the film-forming on the surface of the steel plate and experimental findings of the anti-corrosion inhibition for both samples compared to the control sample due to a unique combination of amine and mercapto type of coupling agents with synergistic effect.

**Keywords:** Cobalt ferrite, Sulfonium group-containing polymer, Coupling agent, Anti-corrosion

## 1. Introduction

Conventionally, when a metal surface is coated, the surface is first degreased, surface treatment is performed and then paint is applied [1]. In recent decades, the National Association of Corrosion Engineers (NACE International) reports estimated the total global cost of corrosion at nearly 3.4% of global GDP (2013) [2]. In the prior art, the surface was first treated with zinc phosphate or chromate to impart anti-corrosion properties to the metal surface and improve adhesion between the surface and the coated film on the surface [3]. On the other hand, in the case of chromate treatment, the chromium in wash water is harmful and can have a detrimental effect on the environment and human beings. This requires expensive wastewater treatment equipment, which is rather uneconomical [6]. However, in the case of zinc phosphate and other phosphate compounds that are extensively used in boilers, the phosphorus contained in the effluent may cause water eutrophication and contamination, and give rise to sludge in the surface treatment bath [4-6]. Until now, few research and methods have been found for forming an organic film or organic/inorganic film based on the polymer nanocolloid prepared based on the



Corresponding author: Behnia sadat Mirhoseini
Email: behniamirhoseini1394@gmail.com

microemulsion system on a metal surface. A microemulsion is defined as a thermodynamically stable isotropic dispersion of two immiscible liquids since the microdomain of either or both liquids have been stabilized by an interfacial film of surface-active molecules [7-13]. In previous methods, treatment of metal surfaces had to be performed while taking precautions against environmental pollution and sludge prevention. These processes require costly effluent treatment/metal surface treatment equipment, which is uneconomical. It is therefore an object of this research, which was confirmed given the above problems in the prior works, to provide a method of forming an organic film or an organic/inorganic composite film having excellent adhesive properties and anticorrosive properties on a metal surface in the surface treatment of metal materials is necessary.

The cubic-spinel-structured $CoFe_2O_4$ ferrite represents a well-known and important class of iron oxide materials. $CoFe_2O_4$ ferrite nanoparticles have been widely studied due to high electromagnetic performance, excellent chemical stability, mechanical hardness, and high cubic magnetocrystalline anisotropy has been widely studied due to high electromagnetic performance, excellent chemical stability, mechanical hardness, and high cubic magnetocrystalline anisotropy [14-16]. Kang et al. [17] investigated the corrosion-protective performance of magnetic $CoFe_2O_4$/polyaniline nanocomposite within epoxy coatings. They confirmed that the carbon steel substrate with the $CoFe_2O_4$-OA-PANI/epoxy coating has the least corrosion depth among others because a denser protective passive layer is formed well on the contact surface between $CoFe_2O_4$-OA-PANI/epoxy coating and carbon steel. The results of 100-day immersion electrochemical impedance spectroscopy under acidic ($9.47 \times 10^{10}$ Ω) or saline ($4.81 \times 10^{10}$ Ω) conditions reveal that the $CoFe_2O_4$-OA-PANI within the epoxy coating has the highest coating resistance, indicating that the $CoFe_2O_4$-OA-PANI is a high-efficiency and highly promising anticorrosive agent for commercial applications. Most of the magnetic properties of $CoFe_2O_4$ ferrite strongly depend on the size and shape of the nanoparticles. It is believed that the microemulsion system is an excellent method to control the size distribution and shape of nanoparticles. Because the monodispersity of nanoparticles for forming a uniform film with high quality is necessary to prevent anti-corrosion damage. To achieve the above object, the film-forming method according to this work is a method comprising a film-forming step wherein a film is formed by bringing an aqueous solution comprising at least one of the following compositions of amino acid and mercapto type of coupling agent into contact with a metal material. A unique combination of lecithin-based surfactant microemulsions that lecithin can act as a surfactant and amino type coupling agent sulfonium group polymer as a mercapto coupling agent and ferrite-based magnetic nanoparticles can act as a new polymer nanocomposite with a synergistic effect to produce a strong film on the surface of the metal with high anti-corrosion activity. In recent years, there has been a need for a film-forming method based on the nanotechnology and polymer colloid materials which does not use surface treatment fluids containing harmful materials such as phosphorus or chromate, does not produce sludge, but which confers excellent anti-corrosion properties.

So, in the current work, the first was prepared. Then by using lecithin-based surfactant microemulsion sulfonium group polymer, styrene, butyl acrylate, and ferrite-based magnetic nanoparticles a new polymer nanocomposite with good particle size and morphology was prepared and characterized with XRD, DLS, and AFM techniques. As an application, the anticorrosion activity of the prepared polymer- composed of ferrite-based magnetite nanoparticles was investigated to prove the role of amine and mercapto-type coupling agents and magnetite nanoparticles for forming the film on the surface of metal compared to control. It is therefore an object of this research, which was conceived given the above problems in the prior art, to provide a method of forming an organic film or a nanocomposite film having excellent adhesive properties and anticorrosive properties on a metal surface.

## 2. Experimental

### 2.1. Materials

High-purity reagents, including Fe $(NO_3)_2 \cdot 9H_2O$, and Co $(NO_3)_2 \cdot 6H_2O$, and NaOH from Merck, were meticulously employed in accordance with their stoichiometric proportions for the synthesis of $CoFe_2O_4$ nanoparticles. Acrylamide undecanoyl oxyphenyl dimethyl sulfonium methyl sulfate was received as gift. Lecithin surfactant and amine type coupling agent, dibutyl fumarate ($C_{12}H_{20}O_4$), styrene monomer ($C_6H_5CH=CH_2$) without any purification, potassium persulfate (KPS) as hydrophilic initiator and HCl were also purchased from Merck.

## 2.2. Synthesis of spinel ferrites via co precipitation method

The co-precipitation method was meticulously implemented to prepare the divalent metal cations magnetic nanoparticles ($MnFe_2O_4$ and $CoFe_2O_4$). The process involved dissolving 16.00 g Fe $(NO_3)_3 \cdot 9H_2O$, and 5.82 g Co $(NO_3)_2 \cdot 6H_2O$ in 200 ml deionized water to create an aqueous precursor solution. Sodium hydroxide was judiciously added dropwise to the solution while maintaining vigorous stirring, ultimately achieving a pH of 13. The reaction was carried out at a constant temperature of 80 °C for 13 h. Subsequent to cooling, the magnetic nanoparticles underwent multiple washing steps with deionized water and ethanol through centrifugation. Finally, the particles were sintered at 800 °C for 3 h [18].

## 2.3. Synthesis of polymer nanocomposite comprising a sulfonium group/$CoFe_2O_4$ nanoparticles core coated by a layer copolymer with a radical-polymerization based on the microemulsion method

50 g water, 0.15 g lecithin as surfactant, 0.1 g spinel ferrites magnetic particles and 0.15 g acrylamide undecanoyl oxyphenyldimethylsulfoniummethylsulfate (AUPDS) were introduced into a three-neck flask fitted with a mechanical stirrer, reflux tube and nitrogen inlet tube, ultrasonically dispersed for 1 h and stirred for 6h. 0.018 g dibutyl fumarate and 0.017 g styrene were added, and the resulting mixture was stirred at 25° C. for 20 h. Next, 0.007 g potassium persulfate (KPS) was added as an initiator, and polymerization was carried out at 60° C. for 24 h in a nitrogen atmosphere at a stirrer speed of 350 rpm. After the reaction, an agglomerate was filtered off by a 200-mesh screen to give a polymer-ferrite nanocomposite and was labeled as PF-A.

## 2.4. Synthesis of polymer nanocomposite comprising a sulfonium group/$CoFe_2O_4$ nanoparticles core coated by a layer copolymer with a radical-polymerization based on the emulsion method

In this section, all experimental were performed based on the above process but in the absence of the lecithin, surfactant to confirm the role of lecithin that acts both surfactant and amine type coupling agent to form a strong film with synergistic effect on the surface of the metal. The prepared polymer-ferrite nanocomposite was also labeled as a PF-B sample.

## 2.5. Film forming based on the dipping/ electrodeposition method

A 10×10×85 mm SPCD steel plate (Nippon steel Co.) (Steel sheets that provide consistent quality and drawing quality second only to that of SPCE.) was dipped in a 2% aqueous solution of degreasing agent (paint protective Coating) at 60 °C for 2 min, rinsed with tap water followed by distilled water (ion exchange water), dried in a current of air. Then the pre-treated plate was dipped in an IPA solution of 1% 3-mercaptopropyltrimethoxysilane ("SH6062", Toray-Dow Co.) for 2 min, and dried at room temperature to give a surface-treated piece. In the film-forming step, the surface-treated piece was dipped in "a nanocomposite colloid for 60 seconds, and a film was formed by electrodeposition by passing a current between a cathode and an anode with the metal material as a cathode. The dipping bath concentration of both nanocomposites PF-A and PF-B concentration were 0.5-5 Wt. %. When the concentration of the above compositions is less than 0.01 Wt. %, the composition of nanocomposite does not easily deposit on the metal surface. Therefore, the film becomes thin, and anticorrosion properties decline. On the other hand, when the concentration of the above composition exceeds 5 Wt. %, an agglomerate deposit during electrodeposition, and a satisfactory film cannot be formed. The current density during electrodeposition was adjusted at 5 $mA/cm^2$. When the current density is less than 0.1 $mA/cm^2$, deposition of any of the compositions on the metal surface is insufficient, and the film becomes thin. On the other hand, when the current density exceeds 10 mA/cm2, the amount of deposition of the compositions of nanocomposite on the metal surface increases but no greater anticorrosion effect is obtained so this is uneconomical. After that, the prepared metal plate was rinsed with tap water and dried in a hot air oven at 120 °C for 5 minutes to give a piece on which a film comprising a polymer nanocomposite with coupling agent was formed.

## 2.6. Monolayer examination by exposure to HCL and anti-corrosion study

Monolayer thin film formation on the surface of metal surface in the presence of prepared polymer-ferrite nanocomposite in lecithin-based microemulsion PF-A sample and lecithin-free emulsion system PF-B sample

with concentration of 1.5 Wt.% were examined by exposure to about a 1.0 M HCl solution for different time intervals from about 1 to 48 h. The inhibition efficiency was calculated as follows:

$$\text{Inhibition efficiency}=W_0\text{-}W_t/W_0\times100 \quad (1)$$

where $W_0$ and $W_t$ were the weight loss of steel plate in absence and in presence of both sample polymer-ferrite nanocomposite of anticorrosive monolayers, respectively. The surface morphology of the formed monolayer was studied using AFM imaging. All experimental test was also studied for control sample in absent of the PF-A and PF-B samples. To study the effect of the anti-corrosion concentration, the experiments were performed with different concentration of PF-A (including 0.5, 1, 1.5, 2, and 2.5 Wt.%) as the best sample with high Inhibition efficiency.

## 2.7. Characterization

The crystal structure of the $CoFe_2O_4$ nanoparticles and polymer- ferrite nanocomposite was analyzed by powder X-ray diffraction (XRD) using an XRD Philips PW1730, with Cu-Kα radiation (λ = 1.5406 Å) and a scanning speed of 10°/s in the $2\theta$ range of 10°–80°. DLS analysis was used to determine the Z-average and particle size distribution histogram using Better size Nanoptic 90. DLS is a fast and non-invasive tool used to measure particle size, size distribution and stability in solutions or suspensions. The film forming on the surface of the steel with both PF-A and PF-B nanocomposite samples was validate with AFM (BRISK).

## 3. Results and discussion

### 3.1. XRD analysis

Fig. 1, shows the XRD patterns of $CoFe_2O_4$ nanoparticles and polymer-ferrite nanocomposite prepared at 180 °C for different reaction times in an autoclave cell with a constant lecithin surfactant based microemulsion system as soft template to control particle size and morphology. The diffraction peaks at $2\theta$ = 30.22°, 35.45°, 43.16°, 53.2°, 57.12°, 62.67°, and 74.3° correspond to (111), (220), (311), (400), (422), (511), (440), and (533) planes, respectively, of the cubic spinel structure of $CoFe_2O_4$ nanoparticles (JCPDS card no. 22-1086) [19]. As can be seen from this Fig.1, and the intensity of peaks, it is clear that the reaction time 13 h, was enough, which means that the crystallinity of $CoFe_2O_4$ nanoparticles also increased. The diffraction peaks at $2\theta$ = 30.22°, 35.45°, 43.16°, 53.2°, 57.12°, 62.67°, and 74.3° was detected in polymer nanocomposite with same pattern but the peak at $2\theta$ = 30.22° shows very low intensity.

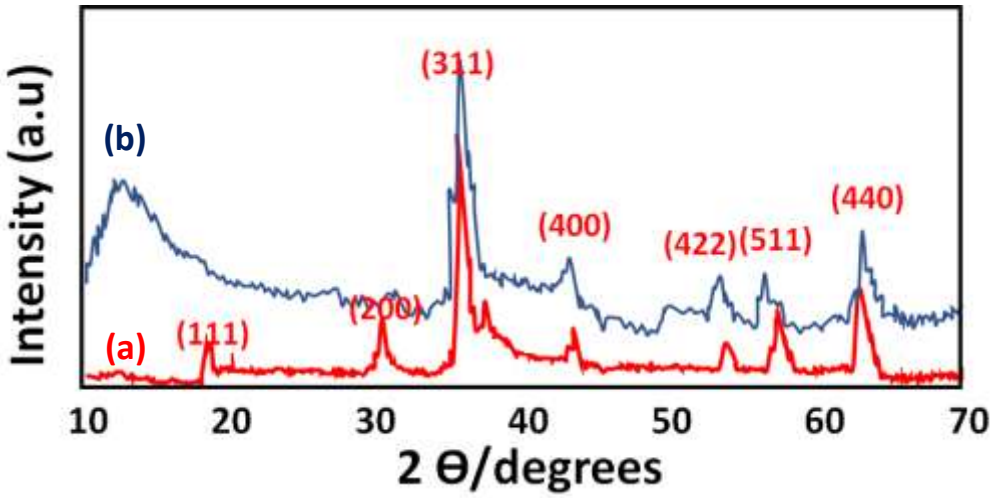


**Fig. 1.** XRD patterns of (a) $CoFe_2O_4$ nanoparticles and (b) polymer-ferrite nanocomposite

### 3.2. DLS study

DLS analysis of polymer-ferrite prepared in lecithin surfactant-based microemulsion and lecithin-free emulsion system are shown in Fig. 2 (a and b). DLS used to measure the size of particles or molecules in a solution is related to the hydrodynamic radius and polydispersity index [20-23]. DLS determines the hydrodynamic size of a nanoparticle in solution by measuring the time scale of Brownian motion. The sample is illuminated with a laser beam, and light waves scattered from the particles interfere constructively and destructively as the particles diffuse randomly. Fig. 2-a shows that the PF-A nanocomposite has a narrow particle size with high monodispersity with (Z-average=45 nanometer) compared to Fig. 2-b with weak monodispersity and (Z-average=277 nanometer). The lecithin that can be used as a surfactant to form nano micelles as a nanoreactor and soft temple provides a condition to control the aggregation of nanoparticles but in a surfactant-free emulsion system the aggregation of nanoparticles is remarkable. Because a colloidal system involves many variables, it can be challenging to control aggregation processes [24-26].

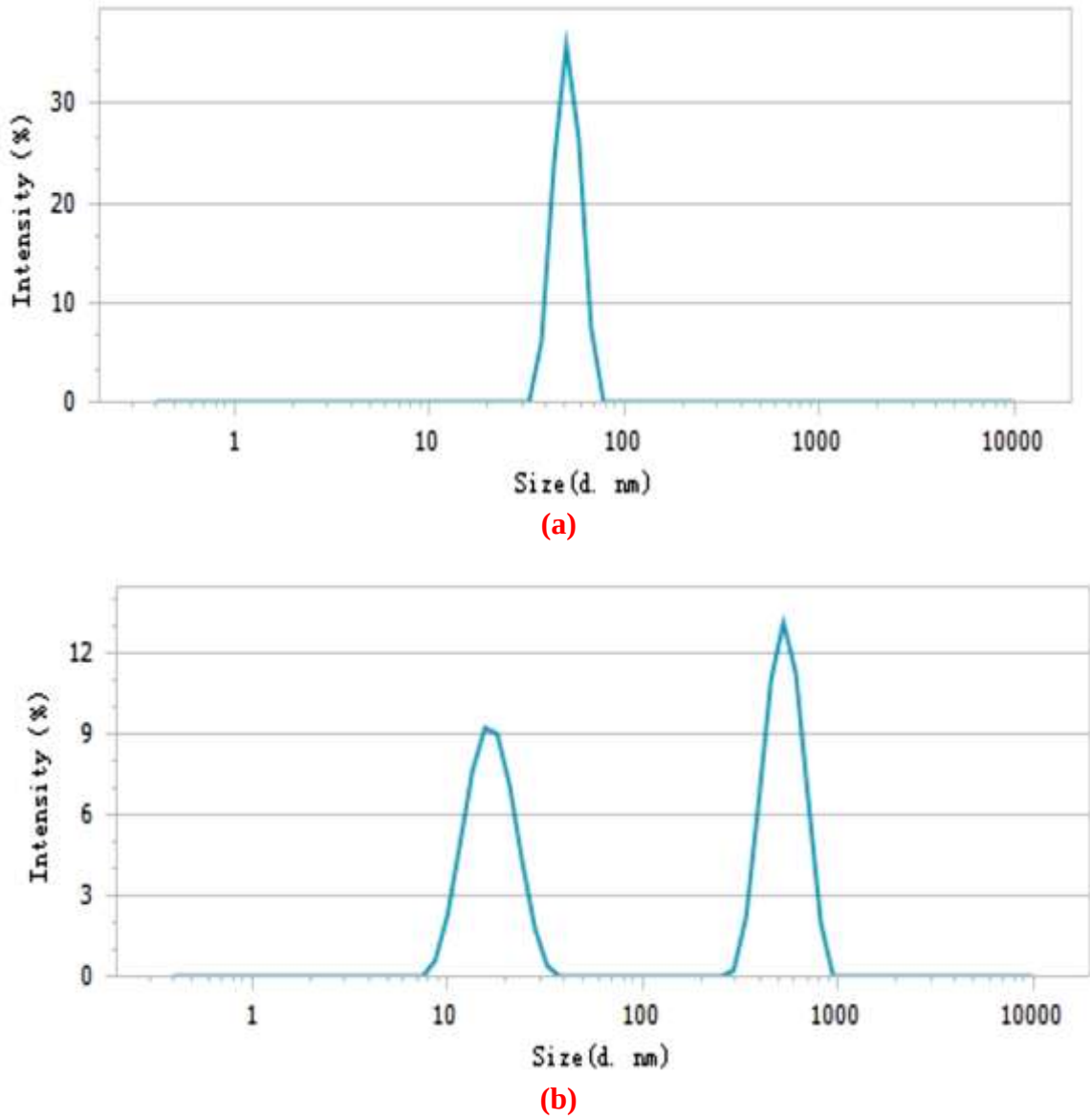


**Fig. 2.** DLS analysis of polymer-ferrite prepared in (a) lecithin surfactant based microemulsion and (b) lecithin free emulsion system.

### 3.3. Anti-corrosion test results

#### 3.3.1. The effect of sample type

Fig. 3, reveals the polymer-ferrite nanocomposite that was prepared in the presence of the lecithin surfactant in a microemulsion system as a soft template [27] FP-A and free lecithin surfactant FP-B and a comparative study without nanocomposite sample as a control sample. From these results, it is clear that according to the film-forming method, a coating with superior anticorrosion properties and adhesion is obtained for both FP-A and FP-B compared to the control sample. Hence, the film-forming method permits an organic film or organic film/inorganic film having superior anticorrosion properties and adhesion to be formed on a metal surface without the use of harmful substances such as phosphorus or chromium compounds. Moreover, sludge is not produced, and an inhibitor effect due to side products may be expected. In this study, both film/inorganic nanocomposites were investigated and PF-A showed superior anticorrosion properties due to the smaller particle size and monodispersity based on the DLS technique. Referring again to the obtained efficiency results the influence of molar HCl exposure on a covered steel surface. Based on the visual observation, the steel surface was damaged and many corrosive punctures appeared all over the surface with PF-B compared to PF-A. It is clear that the globular and monodispersed nanospheres of PF-A with the synergistic effect of amine from lecithin surfactant of mercapto type coupling agent and also narrow nanoparticle size compacted and aligned near each other forming an anticorrosive shield monolayer against the corrosive environment in contrast of the PF-B sample with big and polydispersed nanoparticles.

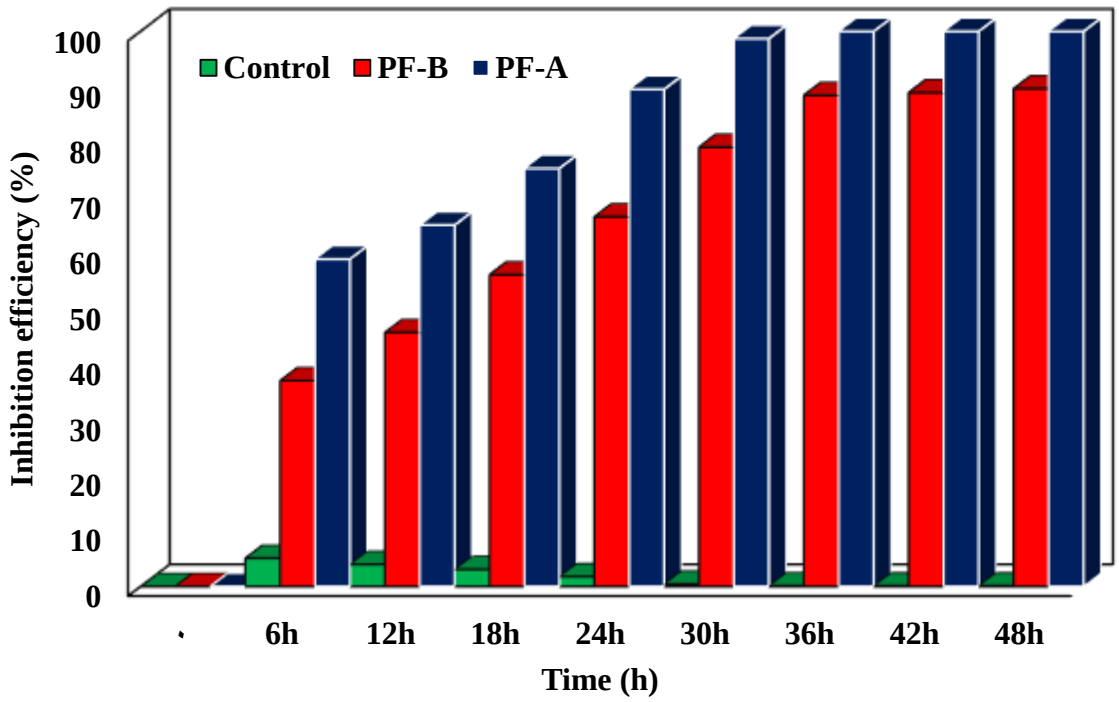


**Fig.** 3. The effect of anticorrosion inhibitor type at room temperature compared to the control sample

Fig. 4, presents a schematic mechanism for film forming on the surface of the steel in the presence of both PF-A and PF-B nanocomposites. AFM images validate that the film forming on the surface with PF-A nanocomposite has uniform and monodispersed nanoparticles. As shown, PF-A nanocomposite with globular nanospheres compacted and aligned near each other forming an anticorrosive shield monolayer compared to the PF-B with polydispersed nanoparticles and AFM analysis confirmed the DLS results. Fig. 5, shows normalized weight loss ($mg/cm^2$) that as can be seen, it is reveal that in the presence of the PF-A nanocomposite, the compacted

anticorrosive shield monolayer formed compared to the PF-B and no weight loss of steel plate after the corrosion test was observed.

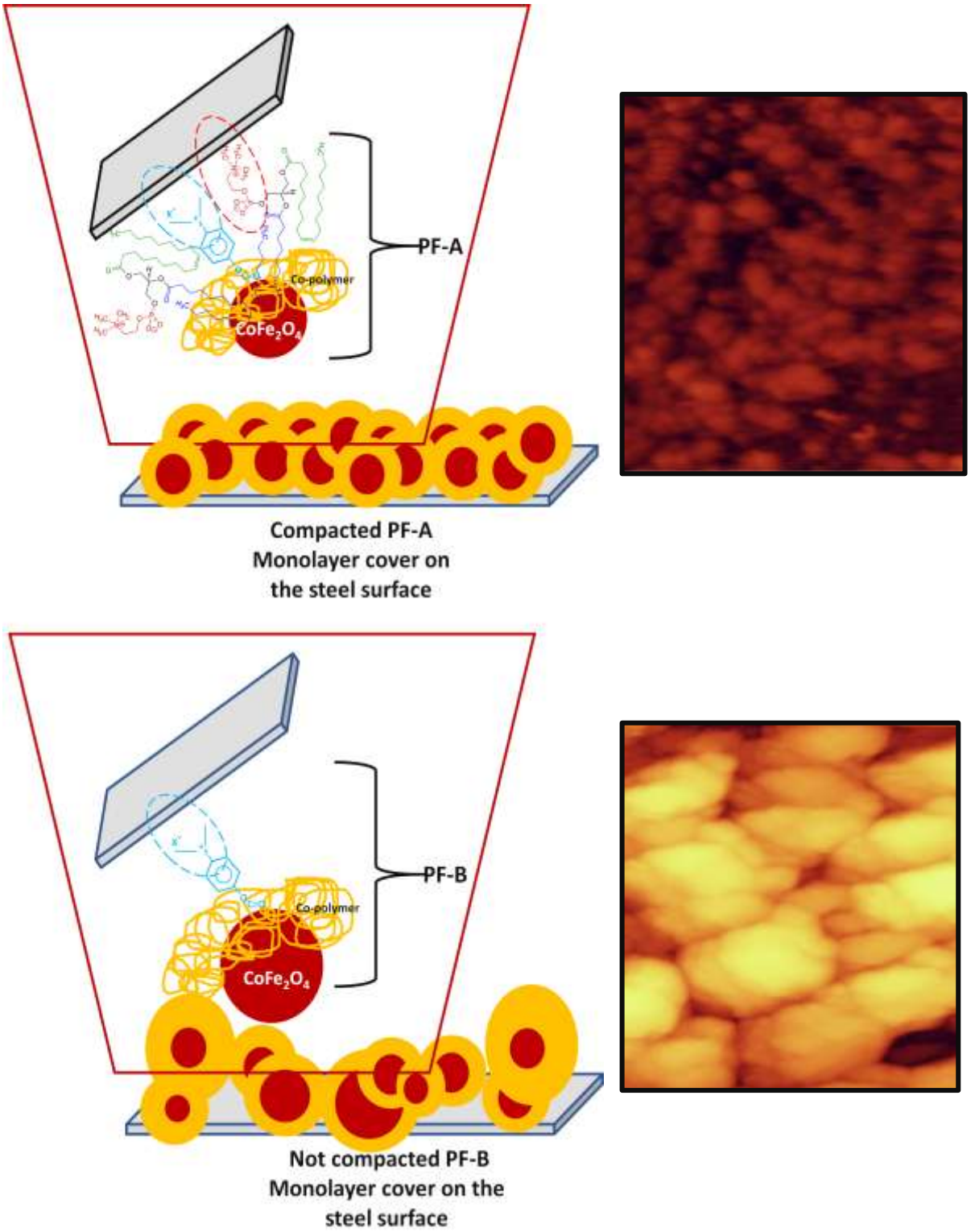


**Fig. 4.** Monolayer film formation on the surface of steel with both nanocomposite samples and related AFM images as a validation technique (scan approach for AFM images was 5μ×5μ).

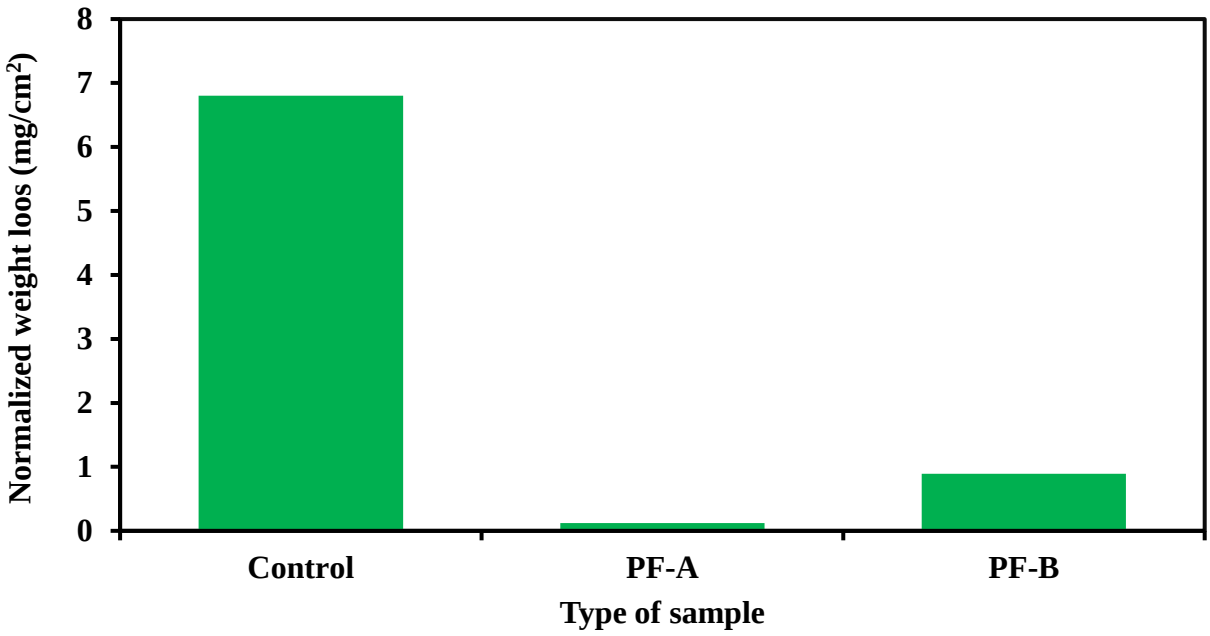


**Fig. 5.** Normalized weight loos measurement of steel plate at room temperature with different polymer-ferrite nanocomposite sample compared to the control sample at room temperature

### 3.3.2. The effect of anticorrosion inhibition concentration

Fig. 6, presents the effect of anticorrosion inhibition concentration at room temperature with PF-A nanocomposite sample. From Fig, which depicts the inhibition efficiency of PF-A nanocomposite monolayer, covering a surface of a substrate increases exponentially at a high reinforced PF-A nanocomposite concentration and then fixed between (0.5-2.5 Wt.%) at room temperature. Such inhibition increases up to 1.0 Wt.% denotes better-orientated monolayer constituents (i.e., charge and reinforced PF-A sample) over the substrate surface, and describes successive building up layer-by-layer of an anticorrosive shield over the substrate surface, hence configuring the surface to resist severe corrosive environments for prolonged periods.

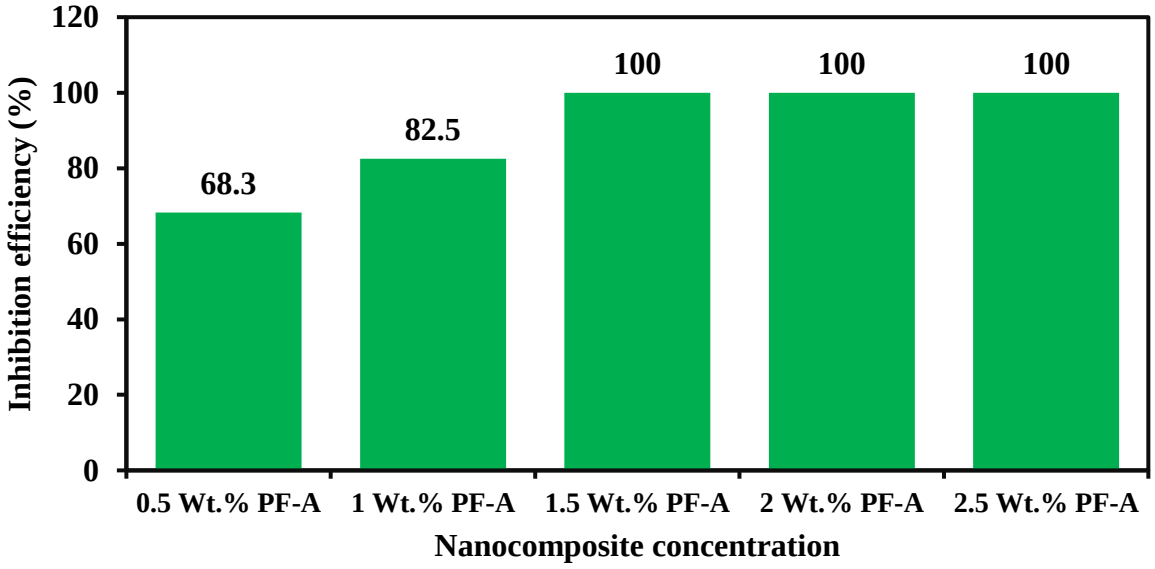


**Fig. 6.** The effect of anticorrosion inhibitor concentration at room temperature with PF-A nanocomposite sample

### 3.3.3. The effect of temperature

The effect of temperature on the inhibition performance at 1.5 Wt.% of PF-A is shown in Fig. 7. As can be seen from Fig. 7, the weight loss of exemplary steel substrate covered by a PF-A monolayer, decreases exponentially at high temperatures.

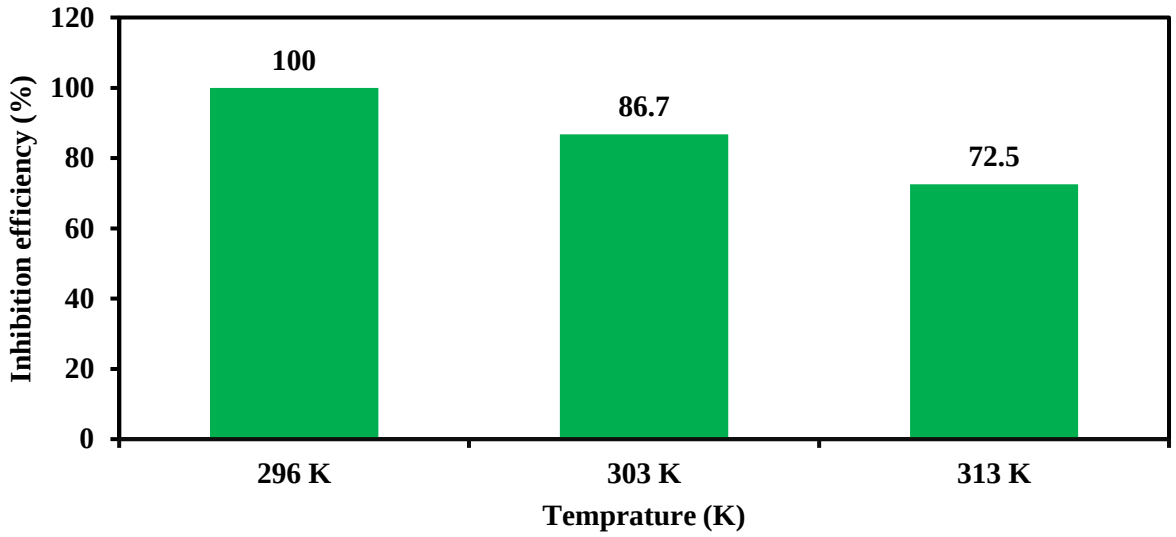


**Fig. 7.** The effect of temperature on the inhibition performance at 1.5 Wt.% of PF-A

### 3.3.4. AFM imaging to confirm the film forming

The AFM image Fig. 8 (a and b) shows a thin film formation of polymer nanocomposite monolayer and covered steel, applied to the steel surface after being exposed to a corrosive HCl solution. In this study, non-contact mode was used. The non-contact mode has the advantage that the tip never makes contact with the sample and therefore cannot disturb or destroy the sample. This is particularly important in corrosion applications. AFM produces surface topography by exploiting the mechanical interaction between the tip and the sample. The tip of the probe is typically a few microns in length and less than 10 nm in diameter. The tip is attached to the free end of a micro-cantilever. The cantilever is approximately 100-200 μm long. According to Hooke's law, when the tip is brought close to the sample surface, the force between the tip and the sample results in a deflection of the cantilever. Depending on the information you are looking for, the force measured in AFM can be different and it includes mechanical contact force, van der Waals force, capillary force, chemical bonding, electrostatic force, magnetic force, and so on. Clearly, for the PF-A-covered surface, globular nanospheres compacted and aligned near each other forming an anticorrosive shield monolayer against the corrosive environment. In the PA-B-covered surface, big-size globular nanospheres with high polydispersity were described schematically in Fig. 4, forming a rough layer on the surface [27]. The strong interaction of inhibitor with the steel surface helps make the surface reaction visible to confirmthe film forming for both samples; in contrast, surface diffusion of adsorbates on metal surfaces for PF-A is often fast on the time scale of the microscope, making identification of film forming simple. These PF-A nanospheres on the surface are present at a much higher density than the PF-B nanostructures seen by AFM images.

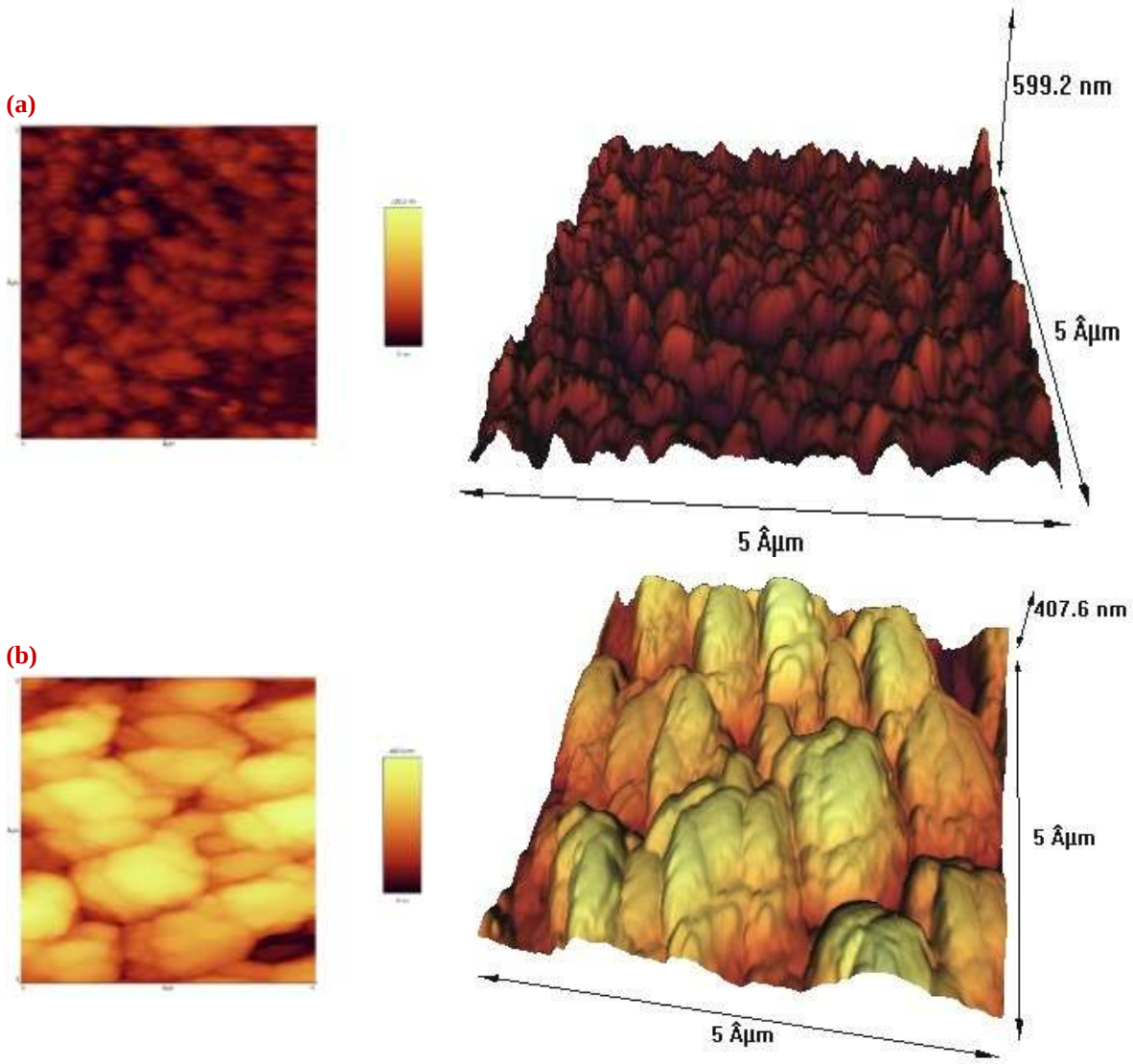


**Fig. 8.** AFM images of (a) compacted PF-A cover and (b) not compacted PF-B cover on the surface.

The AFM image (Fig. 9) described the morphologic changes that occurred over the steel surface after exposure to a corrosive HCl solution in the presence of the optimum concentration of PF-A polymer nanocomposite sample and it can be observed more nanocomposite particles covered the surface. Referring again to Fig. 9, the influence of molar HCl exposure after 48 h on an uncovered steel plate surface and PF-A covered plate. The steel surface in the control sample was damaged and many corrosive punctures appeared all over the surface but in the PF-A covered sample no damage and many corrosive punctures were observed all over the surface. The examination of monolayer firmness against a corrosive 1.0 M HCl environment for about 48 h was visually investigated. The obtained surface reveals no longitudinal and cross-tearing cracks in the surface, and no formation of regular-sized micro-islands in the monolayer was observed. So, no complete disintegration of the anticorrosion film's monolayer was monitored, which reflects the consistency and the firmness of the formed monolayer against a severe acidic environment in the presence of the optimum concentration of the nanocomposite sample. The obtained surface in the presence of PF-B inhibitor reveals longitudinal and cross-tearing cracks in the surface, and the formation of regular-sized micro-islands in the monolayer was observed. The tearing occurs in the weakest points of the monolayer structure as a result of an unsuccessful accumulation of the inhibitor on the covered steel surface with PF-B nanocomposite.

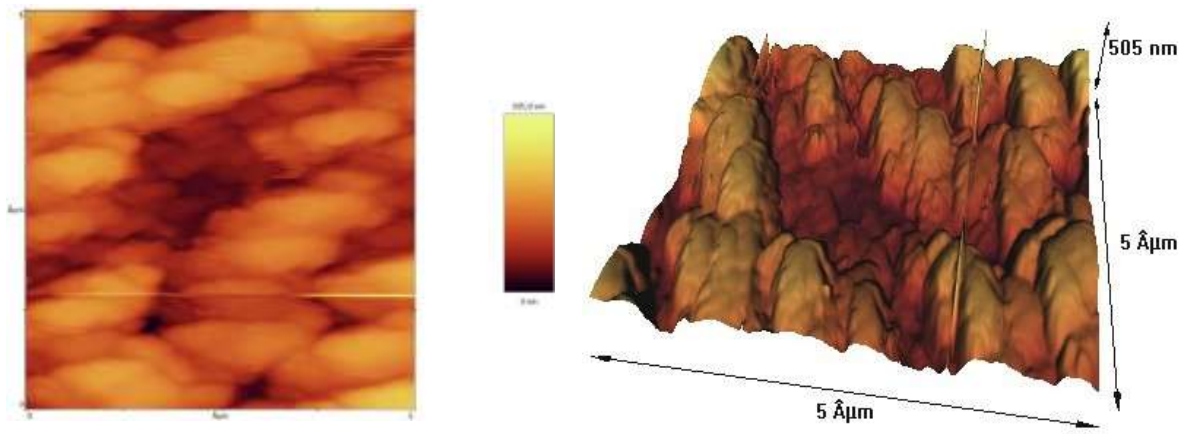


**Fig. 9.** AFM image of the firmness of the formed monolayer against a severe acidic environment in presence of the optimum concentration of PF-A nanocomposite sample

## 4. Conclusion

This study focuses on the combination of amino and mercapto-type coupling agents to fabricate polymer-coated cobalt ferrite nanoparticles for potential application as anti-corrosion. Here, two types polymer-ferrite nanocomposites are composed of a monomer comprising a sulfonium group wherein inorganic nanoparticle cores are coated by a layer comprising a copolymer of the aforesaid monomer at one end of the molecule. Two systems including the lecithin surfactant-based microemulsion system and free lecithin emulsion system were used to synthesize nanocomposites and were labeled as PF-A and PF-B respectively. The prepared samples were characterized with XRD, and DLS analysis. The prepared PF-A nanocomposites provide a forming a film having excellent anticorrosion properties on a metal surface without producing sludge, and without using phosphorus or chromium compared to PF-B in a 1.0 M HCl solution, with 100% maximum corrosion inhibition efficiency at 1.5 Wt.% of nanocomposite compared to the PF-B based on the normalized weight loss (mg/cm$^2$) measurements. The operational parameters such as temperature, and concentration of inhibitor were studied. The film forming on the surface of steel with both nanocomposite samples was confirmed with AFM and obtained results reveal globular nanospheres compacted and aligned near each other forming an anticorrosive shield monolayer against the corrosive environment. AFM images validate the film-forming on the surface of the steel plate and experimental findings of the anti-corrosion inhibition for both samples compared to the control sample due to a unique combination of amine and mercapto-type coupling agents with synergistic effect.

## Acknowledgments

We thank the Boiler Manufacturing Group of Paya Bokhar Markazi Co. (Machine Sazi Arak) for financial support in the form of grants for the research project.

## Conflicts of Interest

The authors declare that they have no known competing financial interests or personal relationships that could have appeared to influence the work reported in this paper.

## Author information

*Corresponding Author: Behnia Sadat Mirhoseini
Email: behniamirhoseini1394@gmail.com

## ORCID

Behnia Sadat Mirhoseini: 0009-0009-7562-5738

## References

[1] S.S. Jamali, D.J. Mills, Steel surface preparation prior to painting and its impact on protective performance of organic coating. Prog. Org. Coat., *77*(12) (2014) 2091–2099. https://doi.org/10.1016/j.porgcoat.2014.08.001

[2] X.Chen, X.G. Li, C.W. Du, Y.F. Cheng, Effect of cathodic protection on corrosion of pipeline steel under disbonded coating. Corrosion Science, 51(9) (900b) 2242–2245. https://doi.org/10.1016/j.corsci.2009.05.027

[3] M. Ghaderi, H. Bi, K. Dam-Johansen, Advanced materials for smart protective coatings: Unleashing the potential of metal/covalent organic frameworks, 2D nanomaterials and carbonaceous structures. Advances in Colloid Interface Sci., 323 (2023) 103055. https://doi.org/10.1016/j.cis.2023.103055

[4] M. Noor Mohammad Beigi, Boosting the impact of cinnamaldehyde-contained polymer microemulsion on the corrosion of C1018 alloy in an acidic medium. Colloid Nanosci. J., 2(1) (2024) 220-227. https://doi.org/10.61186/CNJ.2.1.220

[5] B.S. Mirhoseini, M. Noor Mohammad Beigi, A novel nanocolloid system based on the poly(methyl methacrylate) nanoparticles as anticorrosive agent for boiler; a pilot -scale study. Colloid Nanosci. J., 1(3) (2023) 139-146. https://doi.org/10.61186/CNJ.1.3.139

[6] S. Mishra, R.N. Bharagava, Toxic and genotoxic effects of hexavalent chromium in environment and its bioremediation strategies. J. Environ. Sci. Heal. Part C, 34 (2016) 1–32.

[7] A. Salabat, F. Mirhoseini, F.H. Nouri, Microemulsion strategy for preparation of $TiO_2$–Ag/poly(methyl methacrylate) nanocomposite and its photodegradation application. J. Iranian Chem. Soc. 20 (2022) 599–608. https://doi.org/10.1007/s13738-022-02693-7.

[8] A. Salabat, F. Mirhoseini, K. Abdoli, A microemulsion route to fabrication of mono and bimetallic Cu/Zn/γ-$Al_2O_3$ nanocatalysts for hydrogenation reaction. Scientia Iranica, 25(2018) 1364-1370. https://doi.org/10.24200/sci.2018.5023.1048

[9] F. Mirhoseini, A. Salabata, Iinvestigation of operational parameters on the photocatalytic activity of a new type of poly(methyl methacrylate)/ionic liquid-$TiO_2$ nanocomposite, Iranian J. Chem. Chem. Eng., 38 (2019) 101-114. https://doi.org/10.30492/IJCCE.2019.37613

[10] A. Salabat, F. Mirhoseini, Polymer-based nanocomposites fabricated by microemulsion method, Polym. Compos. 43 (2022) 1282–94.

[11] A. Salabat, F. Mirhoseini, Z. Masoumi, M. Mahdie, Preparation and characterization of polystyrene-silver nanocomposite using microemulsion method and its antibacterial activity, JNS 4 (2014) 377-382.

[12] A. Salabat, F. Mirhoseini, M. Arjomandzadegan, E. Jiryaei, A novel methodology for fabrication of Ag-polypyrrole core-shell nanosphere using microemulsion system and evaluation of its antibacterial application, New J. Chem. 41 (21) (2017) 12892–12900. https://doi.org/10.1039/c7nj00678k

[13] A. Salabat, F. Mirhoseini, M. Mahdieh, H. Saydi, A novel nanotube-shaped polypyrrole-Pd composite prepared using reverse microemulsion polymerization and its evaluation as an antibacterial agent, New J. Chem. 39 (5) (2015) 4109–4114. https://doi.org/10.1039/c5nj00175g

[14] A. Milutinović, Z.Z. Lazarević, M. Šuljagić, L. Andjelković, Synthesis-Dependent Structural and Magnetic Properties of Monodomain Cobalt Ferrite Nanoparticles. Metals, 14(7) (2024) 833. https://doi.org/10.3390/met14070833

[15] A. Salabat, F. Mirhoseini, R. Valirasti, Engineering poly(methyl methacrylate)/$Fe_2O_3$ hollow nanospheres composite prepared in microemulsion system as a recyclable adsorbent for removal of benzothiophene, Ind. Eng. Chem. Research 58 (2019) 17850-1785. https://doi.org/10.1021/acs.iecr.9b04322

[16] F. Kamali, K. Faghihi, F. Mirhoseini, F. High antibacterial activity of new eco-friendly and biocompatible polyurethane nanocomposites based on $Fe_3O_4$/Ag and starch moieties. Polym. Eng. Sci., 62(5) (2022) 1444-1462.https://doi.org/10.1002/pen.25934

[17] Y.-T. Kang, C.-C. Wang, C.-Y. Chen, Corrosion-protective performance of magnetic CoFe2O4/polyaniline nanocomposite within epoxy coatings. J. Taiwan Inst. Chem. Eng., 127 (2021) 357–366. https://doi.org/10.1016/j.jtice.2021.08.008

[18] Shakeel V, Hussain Gul I, John P, Bhatti A. Biocompatible gelatin-coated ferrite nanoparticles: A magnetic approach to advanced drug delivery. Saudi Pharm J. 2024, 32(6):102066. doi: 10.1016/j.jsps.2024.1020665

[19] Duong HDT, Nguyen DT, Kim K-S. Effects of Process Variables on Properties of $CoFe_2O_4$ Nanoparticles Prepared by Solvothermal Process. *Nanomaterials*. 2021;

[20] F. Mirhoseini, Alireza Salabat, Ionic liquid based microemulsion method for fabrication of poly(methyl methacrylate)–$TiO_2$ nanocomposite as highly efficient visible light photocatalyst, RSC Adv. 5 (2015) 12536–12545. https://doi.org/10.1039/c4ra14612c

[21] A. Salabat, F. Mirhoseini, Applications of a new type of poly(methyl methacrylate)/$TiO_2$ nanocomposite as an antibacterial agent and a reducing photocatalyst. Photochem. Photobiol. Sci., 14(9) (2015) 1637–1643. https://doi.org/10.1039/c5pp00065c

[22] F. Mirhoseini, A. Salabat, (2018). Removal of methyl tert -butyl ether as a water pollutant by photodegradation over a new type of poly(methyl methacrylate)/$TiO_2$ nanocomposite. Polymer Composites, *39*(4) (2018) 1248–1254. https://doi.org/10.1002/pc.24059

[23] F. Mirhoseini, A. Salabat, Antibactrial activity based poly(methyl methacrylate) supported $TiO_2$ photocatalyst film nanocomposite, Tech. J. Eng. Appl. Sci. 5 (2015)115-118.

[24] A. Salabat, B.S. Mirhoseini, F. Mirhoseini, Ionic liquid based surfactant-free microemulsion as a new protocol for preparation of visible light active poly(methyl methacrylate)/$TiO_2$ nanocomposite. Sci Rep 14, 15676 (2024). https://doi.org/10.1038/s41598-024-66872-7

[25] F. Mirhoseini, A. Salabat, Polymer nanocomposite based composition and method for controlling water hardness, United States patent 11136247.

[26] F. Mirhoseini, A.Salabat, Photocatalytic filter, United States patent 10828629.

[27] F. Mirhoseini, B.S. Mirhoseini, M. Noor Mohammad Beigi, M. Understanding the photodegradation of amoxicillin antibiotic using visible light sensitized poly(methyl methacrylate)/$TiO_2$ nanocomposite. *Nano Sci. Technol. J.* 1(1) (2023) 38-48. https://doi.org/10.22034/nstj.2023.707804

[28] M. Hoseini, S. Hamidi, E. Salehi, A. Mohammadi, F. Mirhoseini, M. Ravaghi. Multi-variate multi-objective optimization of production conditions for electro-spun skin scaffold using RSM and investigation of gamma irradiation effects on the properties of the optimized sample. Heliyon 10 (12) (2024a) e3294.

[28] A. Salabat, F. Mirhoseini, Photo-induced hydrophilicity study of poly(methyl methacrylate)/$TiO_2$ nanocomposite prepared in ionic liquid based microemulsion system. Current Appl. Polym. Sci., 2(2), (2018) 112–120. https://doi.org/10.2174/2452271602666180803141554